HHS Public Access

Author manuscript

Int J Pharm. Author manuscript; available in PMC 2020 September 10.

Published in final edited form as:

Int J Pharm. 2019 September 10; 568: 118504. doi:10.1016/j.ijpharm.2019.118504.

Correlations between surface composition and aerosolization of jet-milled dry powder inhaler formulations with pharmaceutical lubricants

Sharad Mangal[1,6], **Heejun Park**[1,6], **Reham Nour**[1], **Nivedita Shetty**[1], **Alex Cavallaro**[2], **Dmitry Zemlyanov**[3], **Kyrre Thalberg**[4], **Vibha Puri**[5], **Mark Nicholas**[4], **Ajit S. Narang**[5], **Qi (Tony) Zhou**[1,*]

[1]Department of Industrial and Physical Pharmacy, College of Pharmacy, Purdue University, 575 Stadium Mall Drive, West Lafayette, IN 47907, USA

[2]Future Industries Institute, University of South Australia, Mawson Lakes, SA 5095, Australia

[3]Birck Nanotechnology Center, Purdue University, West Lafayette, IN 47907, USA

[4]Inhalation Product Development, Pharmaceutical Technology & Development, AstraZeneca, Gothenburg, Sweden

[5]Small Molecule Pharmaceutics Department, Genentech, Inc., One DNA Way, South San Francisco 94080, CA, USA

[6]These authors contribute equally to the study

Abstract

Co-jet-milling drugs and lubricants may enable simultaneous particle size reduction and surface coating to achieve satisfactory aerosolization performance. This study aims to establish the relationship between surface lubricant coverage and aerosolization behavior of a model drug (ciprofloxacin HCl) co-jet-milled with lubricants [magnesium stearate (MgSt) or L-leucine]. The co-jet-milled formulations were characterized for their particle size, morphology, cohesion, Carr's index, and aerosolization performance. The surface lubricant coating was assessed by probing surface chemical composition using X-ray photoelectron spectroscopy (XPS) and time-of-flight secondary-ion mass spectrometry (ToF-SIMS). The effects of co-jet-milling on the surface energy and *in vitro* dissolution of ciprofloxacin were also evaluated. Our results indicated that, in general, ciprofloxacin co-jet-milled with L-leucine at > 0.5% w/w showed a significant higher fine particle fraction (FPF) compared with the ciprofloxacin jet-milled alone. The FPF values plateau at or above 5 % w/w for both MgSt and L-leucine. We have established the quantitative correlations between surface lubricant coverage and aerosolization in the tested range for each of the

[*]**Corresponding Author:** Qi (Tony) Zhou, Tel.: +1 765 496 0707, Fax: +1 765 494 6545, tonyzhou@purdue.edu.

Declaration of interests

The authors declare that they have no known competing financial interests or personal relationships that could have appeared to influence the work reported in this paper.

lubricants. More importantly, our results suggest different mechanisms to improve aerosolization for MgSt-coating and L-leucine-coating, respectively: MgSt-coating reduces inter-particulate interactions through the formation of low surface energy coating films, while L-leucine-coating not only reduces the surface energy but also creates rough particle surfaces that reduce inter-particulate contact area. Furthermore, surface coatings with 5% w/w MgSt (which is hydrophobic) did not lead to substantial changes in *in vitro* dissolution. Our findings have shown that the coating structure/quality and their effects could be highly dependent on the process and the coating material. The findings from this mechanistic study provide fundamental understanding of the critical effects of MgSt and L-leucine surface coverages on aerosolization and powder flow properties of inhalation particles.

Graphical Abstract

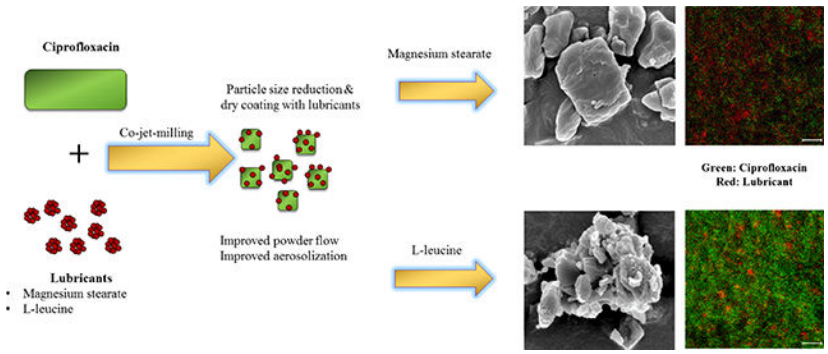

Keywords

Dry powder inhaler; lubricant; aerosol performance; jet-milling; surface composition; high-dose

1. Introduction

Inhalation is an established route for administering drugs directly to the lungs (Frijlink and De Boer, 2004). Compared with the systemic therapies for pulmonary diseases, inhalation therapies may provide more rapid clinical response with relatively lower doses while reducing the risk of systemic side effects (Cipolla and Chan, 2013). For instance, inhaled antibiotic therapies have been increasingly used for treatment of respiratory infections (Zhou et al., 2015). Delivering antibiotics to the lungs in an optimal concentration is central to effective treatment of such infections (Hickey et al., 2016; Velkov et al., 2015). However, for some antibiotics such as colistin, only small and often ineffective fractions of orally or parenterally administered antibiotics reach the infection sites at the lung surface (Cheah et al., 2015). Inhalation therapies of several antibiotics have been shown to achieve a much higher drug concentration on the airway surface as compared with oral or intravenous administration (Lin et al., 2017a; Lin et al., 2018; Lin et al., 2017b).

Dry powder inhalers (DPIs) are popular for delivery of high-dose antibiotics as exemplified by TOBI® Podhaler® (tobramycin) (Miller et al., 2015) and Colobreathe® (colistimethate sodium) (Schwarz, 2015). Jet-milling is the mainstay industrial approach to produce drug

particles within the inhalable size range for DPIs (Lin et al., 2015; Pilcer and Amighi, 2010). However, jet-milled powders are often highly cohesive and exhibit poor aerosolization efficiency and flowability (Jong et al., 2016; Lin et al., 2015; Telko and Hickey, 2005). To improve the aerosolization and flow, cohesive jet-milled drug powders are blended with relatively large carrier particles, typically lactose (Chan and Chew, 2003; Kou et al., 2012). This requires large amounts of carrier particles, which in the case of antibiotics, would lead to inhalation of large amounts of powder. Such high powder load may make the multi-dose inhaler very large and increase the number of inhalations to complete the dose (Zhou et al., 2014). Thus, minimizing the use of excipients is an important factor to minimize the required patient effort and, thereby, to maximize patient compliance and adherence, especially for high-dose DPIs (Healy et al., 2014).

Previous studies have suggested that the coating of cohesive particles with lubricants can improve the aerosolization of inhalable powders at a low excipient concentration (Zhou et al., 2013; Zhou et al., 2010). This is typically achieved by processing milled inhalable powders with lubricants using specialized dry coating equipment such as mechanofusion, which facilitates efficient coating of lubricant particles over host particles (Zhou et al., 2013; Zhou et al., 2010). Recently, co-jet-milling with lubricants was shown to simultaneously facilitate particle size reduction and particle surface coating, which resulted in improved aerosolization performance (Lau et al., 2017a, b; Morton and Staniforth, 2005; Morton et al., 2005; Musa et al., 2000; Staniforth et al., 2004; Stank and Steckel, 2013; Steckel and Stank, 2014). This approach is relatively simple compared with the traditional two-step milling/dry coating approach, as powders may be micronized and dry coated in a single-step. It reduces the need for powder handling and processing and may be amenable to a continuous manufacturing process (Lau et al., 2017b).

Surface coating with lubricants such as magnesium stearate (MgSt) (Giry et al., 2006; Morton and Staniforth, 2005) and L-leucine (Staniforth et al., 2004) has been shown to improve the aerosolization efficiency of cohesive drug particles. MgSt has been approved to use in DPI products such as Breo Ellipta. Although L-leucine has not been approved for inhalation products, it has been widely employed in DPI research, and L-leucine is endogenous to the body. The level of coating achieved with lubricants plays a pivotal role in aerosolization (Zhou et al., 2013). Earlier studies have shown different lubricants may have different coating efficiency (Wei et al., 2017). For example, mechanofusing ibuprofen particles with MgSt led to relatively smoother surface coating, while L-leucine coating resulted in flake-like coating patterns (Qu et al., 2015b). However, as far as we know, the quantitative correlations between surface coating coverage of MgSt and L-leucine and aerosolization performance of the powders co-jet-milled with lubricants have not been established. Therefore, such potential correlations were examined here systematically.

In this study, ciprofloxacin was selected as a model drug because it is a common antibiotic for lung infections, which is in the late development stage as a DPI product (Antoniu and Azoicai, 2013). Here ciprofloxacin was co-jet-milled with different lubricants (MgSt and L-leucine) at various process conditions (feed and grinding pressures and number of jet-milling cycles). The concentrations of coating materials were selected based on a previous report on dry coating of fine micronized particles (Zhou et al., 2013). MgSt has been approved for

inhalation products such as ELLIPTA® DPIs. However, the amount of MgSt in the DPI formulation should be minimized to avoid safety concerns. Although L-leucine has not be approved for commercial inhalation products, it is an endogenous material and has been widely used in DPI research (Begat et al., 2005; Mangal et al., 2018). The surface composition of co-jet-milled powders was examined using X-ray photoelectron spectroscopy (XPS) and Time-of-flight secondary-ion mass spectrometry (ToF-SIMS). Impacts of degree of coating on the surface energy, cohesion, Carr's index, and *in vitro* aerosolization and dissolution were also evaluated. We correlated the surface lubricant coverages with the aerosolization of the co-jet-milled powders for a better fundamental understanding of dry powder inhaler formulations.

2. Materials and Methods

2.1 Materials

Ciprofloxacin hydrochloride monohydrate (ciprofloxacin) was purchased from Beta Pharma (Shanghai) Co. Ltd, Wujiang City, JiangSu Province, China. Acetonitrile (HPLC grade) was purchased from Merck (Fair Lawn, New Jersey, USA), MgSt from Mallinckrodt Pharmaceuticals (Mallinckrodt Pharmaceuticals, St. Louis, Missouri, USA) and L-leucine from Sigma-Aldrich (St. Louis, Missouri, USA). L-leucine was milled to achieve similar particle size to that of MgSt (8–10 μm) using a ball mill (8000M Mixer/Mill, SPEX CertiPrep, New Jersey, USA) with 20 methacrylate balls (diameter, 3.18 mm) at 1080 cycles/min for 10 min.

2.2 Jet-milling

An initial blend of ciprofloxacin and lubricants (MgSt or L-leucine) was gently stirred for 5 min with a mortar and pestle. The resultant blends (~500 – 800 mg) were co-milled using a jet-mill (Piconizer spiral jet-mill, Hosokawa Alpine AG, Augsburg, Germany), at a feed rate of 1 g/min. The effects of grinding and feed pressures and the number of jet-milling cycles on aerosolization were investigated. The co-milled samples were stored in glass containers under the desiccated conditions (RH < 20%).

2.3 Scanning electron microscopy (SEM)

Morphology of selected formulations was evaluated by a SEM (FE-SEM, NOVA nanoSEM, FEI Company, Hillsboro, Oregon, USA). The powder sample was dispersed on a sample stub mounted with an adhesive carbon tape. The excess powder was removed with the help of pressurized air and then coated with platinum at 40 mA for 1 min using a sputter coater, which created a coating with thickness of approximately 10 – 20 nm (208 HR, Cressington Sputter Coater, England, UK).

2.4 Particle size distribution

Particle size distribution of the selected jet-milled samples was determined by laser diffraction using a Mastersizer 3000 with an Aero-S dry powder dispersion unit (Malvern Instruments, Worcestershire, UK). Each powder sample (approximately 10 – 20 mg) was fed into the dispersion system. Compressed air at 4 bar was used to disperse the powder through

the measuring zone. D_{10}, D_{50} and D_{90} were calculated using built-in software. Span was calculated as $(D_{90} - D_{10})/D_{50}$.

2.5 Time-of-flight secondary-ion mass spectrometry (ToF-SIMS)

Surface distributions of lubricant were mapped using time-of-flight secondary-ion mass spectrometry (ToF-SIMS, nanoToF instrument, Physical Electronics Inc., Chanhassen, MN, USA) at 30 kV. For mapping purposes, signals were collected from an area of approximately 90 μm × 90 μm for each sample. Characteristic peak fragments were identified to effectively distinguish ciprofloxacin from lubricant materials: for ciprofloxacin, m/z ~ 332, corresponding to the fragment $[C_{17}H_{19}FN_3O_3^+]$; for MgSt, m/z 24 corresponding to the fragment $[Mg^+]$; and for L-leucine, m/z 132 corresponding to the fragment $[C_6H_{14}NO_2^+]$.

2.6 X-ray photoelectron spectroscopy (XPS)

The surface composition was quantitatively evaluated using X-ray photoelectron spectroscopy (XPS) (AXIS Ultra Imaging DLD spectrometer, Kratos Analytical Inc., Manchester, UK) (Zhou et al., 2011). The instrument was equipped with monochromic Al Kα radiation (1486.6 eV) and was operated at a constant pass energy (PE) of 20 eV (allows resolution of ~0.35 eV) and 160 eV for high-resolution and survey spectra, respectively. A built-in commercial Kratos charge neutralizer was used to avoid non-homogeneous electric charge on the analysed powders (all of which were non-conductive) and to achieve better resolution.

Binding energy (BE) values refer to the Fermi edge, and the energy scale was calibrated using Au $4f_{7/2}$ at 84.0 eV and Cu $2p_{3/2}$ at 932.67 eV. The XPS data were analysed with CasaXPS software. The C-C component of the C 1s peak was set to a binding energy of 284.8 eV to correct for charge on each sample/acquisition point. Model C 1s spectra obtained from pure compounds were used as input for curve-fitting following subtraction of Shirley background (Bhujbal et al., 2018). The atomic concentrations of the elements in the near-surface region (typically ~5–10 nm) were estimated after a Shirley background subtraction, taking into account the corresponding Scofield atomic sensitivity factors and inelastic mean free path (IMFP) of photoelectrons using standard procedures in the CasaXPS software.. The XPS measurement spot is a circle approximately 0.5 mm in diameter. Six replicates were measured for each sample.

2.7 Surface energy analysis

The surface energies of the samples were examined by a surface energy analyzer based on inverse gas chromatography (iGC-SEA, Surface Measurement Systems Ltd., London, UK) following the procedure described earlier with slight modifications (Das et al., 2011; Yla-Maihaniemi et al., 2008). Prior to the measurement, samples were stored in a desiccated chamber with RH < 20%. Approximately 300 mg of powder was gently packed into a pre-silanized glass column (300 mm × 4 mm) without subjecting to excessive tapping to avoid consolidation. Both ends of the columns were loosely filled with silanized glass wool to avoid powder movement. Prior to measurements, pre-conditioning of the column was

conducted with helium at 10 standard cubic centimetre per minute (sccm) for 60 min at 303 K and 0% RH.

Dispersive energy was measured using n-alkanes (decane, nonane, octane, heptane and hexane), while the specific surface energy was measured using acidic (dichloromethane) and basic (ethyl acetate) probes. The surface energy was measured at various fractional surface coverages between 0.01 and 0.08 p/p_0 (where p is the partial pressure and p0 is the saturation vapour pressure). Helium at a flow rate of 10 sccm maintained at 303 K at 0% RH was used to carry the probes through the columns. Dispersive surface energy was calculated as described by Schultz (Schultz et al., 1987). The specific surface energy was calculated by the following equation (van Oss et al., 1987).

$$\gamma^{ab} = \sqrt{\gamma_S^+ \gamma_S^-} \quad \text{Eq. (1)}$$

Here, γ_S^+ represents the acidic component, and γ_S^- represents the basic component of surface energy. The total surface energy ($\gamma;^T$) is the sum of the dispersive ($\gamma;^D$) and specific ($\gamma;^{ab}$) components (Fowkes, 1964). Triplicates for each powder formulation were conducted.

2.8 Carr's index

Powder samples (~500 mg) were gently poured into a 10 mL measuring cylinder, and the volume was measured. Then the cylinder was tapped for 2000 taps (no further consolidation), and the tapped volume was measured. Four replicates were conducted for each sample. The following equation was used to calculate the Carr's index (Carr, 1965):

$$Carr's\ Index = \frac{\rho_T - \rho_B}{\rho_T} \times 100 \quad \text{Eq. (2)}$$

2.9 Shear cell

The cohesion of the jet-milled samples was measured by an FT4 powder rheometer (Freeman Technology Ltd., Worcestershire, UK). Approximately 300 – 500 mg of powder was transferred into a 1 mL shear cell module. The powder was then conditioned using a conditioning blade. The normal stresses of 3, 4, 5, 6 and 7 kPa were applied to the powder, and shear stress was measured at each normal stress. The maximum shear stress that the powder bed can support under given normal stresses represents the yield loci (Schulze, 2008). The yield loci at zero normal stress represents cohesion, which is calculated according to the equation below (Schulze, 2008):

$$C = \tau - \sigma \tan\eta \quad \text{Eq. (3)}$$

where, τ represents the shear stress, σ represents the normal stress, η represents the angle of friction, and C represents the cohesion. Four replicates were conducted for each sample.

2.10 Drug quantification

Concentrations of ciprofloxacin were determined using an established HPLC method (Shetty et al., 2018). An Agilent HPLC system with an Agilent Eclipse Plus column (5 μm C18 150 × 4.60 mm) were used for drug analysis (Agilent, Waldbronn, Germany). The mobile phase is a mixture of: (A) 76% v/v of 30 mM Na_2SO_4 (adjusted to pH 2.5 with H_3PO_4); and (B) 24% w/w of acetonitrile. The isocratic program was set for 4 min at the flow rate of 1.0 mL/min and a wavelength of 215 nm. The calibration curve for ciprofloxacin was linear (r^2 > 0.999) in the range of 0.004–0.125 mg/mL.

2.11 *In vitro* aerosol efficiency

The aerosolization performance of powder samples was evaluated by a Next Generation Impactor (NGI, Apparatus X, USP X, Copley, Nottingham, UK). To minimize particle bounce, the stages (1–8) of the impactor were coated with silicone grease. The powder (10 ± 2 mg) was filled into the capsule (size 3 hydroxypropyl methylcellulose capsules, Qualicaps, Whitsett, NC, USA), and two capsules were dispersed through an RS01 DPI device (similar design to Osmohaler, Plastiape S.p.A., Osnago, Italy) following a standard dispersion procedure (USP 38). The dispersion was carried out at an airflow of 100 L/min for 2.4 s allowing a total of 4 L of air to pass through the inhaler with a pressure drop of approximately 4 kPa (Wang et al., 2016). Drug deposition on capsule, inhaler device, USP throat and stages 1–8 of the impactor was collected using 20 mL of water. Fine particle fraction (FPF) was defined as the proportion of the total recovered drug with an aerodynamic diameter smaller than 5 μm.

2.12 *In vitro* dissolution

The dissolution studies were carried out on aerodynamically classified particles collected on stage 4 of NGI (Mangal et al., 2018). The studies were carried out using 20 mL of degassed phosphate buffer saline (PBS) at pH 7.4 as dissolution medium. PBS has been used widely as a simple dissolution medium for inhalation formulations in the literature (May et al., 2012; Salama et al., 2008). Two capsules (size 3 hydroxypropyl methylcellulose capsules, Qualicaps, Whitsett, NC, USA) each containing 5 ± 1 mg of the formulation were dispersed through an RS01 inhaler using the same protocol as above. The powder under the jet of stage 4 of the NGI was collected on a filter paper disk (Whatman® Grade 2, pore size 5 μm, GE Healthcare) for dissolution studies. An aliquot of sample (0.2 mL) was taken at selected time intervals (2, 5, 10, 15, 20, 30, 45, 60, 90, 120, 150 and 180 min); then an equal volume of fresh medium was added. As there is no regulatory guideline on dissolution tests for orally inhaled powder products, two common dissolution methods were employed: beaker and Franz cell methods (Mangal et al., 2019).

2.12.1 Beaker method—The aerosol fraction collected on the filter disk was placed in 100 mL beakers (4.7 mm internal diameter × 8.5 cm high, Vineland, NJ, USA) containing 20 mL of the dissolution media maintained at 37 °C. The medium was stirred at 500 rpm (VWR International, Arlington Heights, IL, USA) with the help of a polygon magnetic bar (12 mm, VWR International, Arlington Heights, IL, USA).

2.12.2 Franz cell method—Filter disks with the aerosol powder were placed on the Franz cell. Care was taken to ensure that an air bubble was not trapped under the filter disk during this operation. The Franz cell (V6B, PermeGear Inc., Hellertown, PA, USA) reservoirs were filled with 20 mL of the dissolution medium maintained at 37 °C. The medium was stirred at a fixed speed of 600 rpm (6-station Franz Cell stirrer, PermeGear Inc., Hellertown, PA, USA).

2.13 Statistical analysis

One-way analysis of variance (ANOVA) with Tukey post-hoc test was used for statistical analysis of three groups or more by a GraphPad Prism software (GraphPad Software, Inc., La Jolla, CA, USA). Independent T-test was used for comparing two groups. The asterisks over graphs indicated the statistical differences where * = $p < 0.05$, ** = $p < 0.01$, *** = $p < 0.001$, and NS denotes $p > 0.05$.

3. Results

3.1 Particle size

Table 1 shows the particle sizes of the selected ciprofloxacin jet-milled formulations. The jet-milled ciprofloxacin formulations had D_{50} of < 2 μm and D_{90} < 5 μm. The particle sizes of ciprofloxacin co-jet-milled with different lubricants were similar to that for the jet-milled ciprofloxacin alone. Thus, the differences in the aerosolization performance of these powders are unlikely to be the consequence of changes in particle size.

3.2 *In vitro* aerosolization

Effect of coating material concentrations—MgSt and L-leucine were selected to investigate the effect of lubricant concentration on the aerosolization of ciprofloxacin. Ciprofloxacin jet-milled alone showed an FPF of 62.1 ± 0.9 (Figure 1A). Co-jet-milling with L-leucine substantially improved the FPF of ciprofloxacin. The improvement was notable even at a very low lubricant concentration of 0.5% w/w of L-leucine. Co-jet-milling with MgSt also resulted in a significant increase in FPF at 5% w/w and higher. The FPF values plateaued at 5% lubricant for both L-leucine and magnesium stearate; further increases in lubricant concentration to 10% w/w showed no improvement in FPF as compared with that of 5% w/w of lubricants.

3.3 Time-of-flight secondary-ion mass spectrometry (ToF-SIMS)

Figure 2 shows the spatial distribution of lubricants (red) on the surfaces of co-jet-milled ciprofloxacin particles (green). The images of the ciprofloxacin co-jet-milled with 0.5% w/w of lubricants showed that very few areas of the particle surfaces were covered by the lubricants. The amount of lubricants on the surface increased with an increase of lubricant concentration in the formulation. The intensity of red signals (for the lubricants) in the images was greater for MgSt as compared with the same concentration of L-leucine, suggesting that the coating quality varies with different lubricants. We have performed XPS tests to confirm this finding, see below.

3.4 X-ray photoelectron spectroscopy (XPS)

Surface coverage of lubricants on the co-jet-milled particles was further quantified using XPS (Table 2). The theoretical % surface coverage represents the percentage of carbon atoms from each molecule as determined from their molar composition, with an assumption that drugs and lubricants exist as the physical mixture without coating effects. The results show that MgSt achieved greater lubricant surface coverage than L-leucine at the 5% and 10% lubricant levels. This confirms the qualitative results shown in the ToF-SIMS images of Figure 2. For instance, with 5% w/w lubricant, the surface concentration was 32.7 ± 4.8 for MgSt but was only 15.0 ± 4.9 for L-leucine.

3.5 Surface energy analysis

The jet-milled ciprofloxacin alone had the highest surface energy (dispersive, specific and total) values over the entire fractional coverage range ($p < 0.05$). Co-jet-milling with L-leucine and MgSt substantially reduced the total surface energy of the resulting blend (Figure 3). The surface energy of ciprofloxacin reduced with increasing concentration of MgSt (Figure 3) but remained relatively unchanged with varying L-leucine concentration (Figure 3). Interestingly, despite the higher surface coverage and lower surface energy, the FPF achieved with 5% MgSt was lower than that achieved with the corresponding concentration of L-leucine.

3.6 Scanning electron microscopy (SEM)

Representative SEM images of the selected samples are shown in Figure 4. Raw ciprofloxacin appeared as large rod-shaped particles (Figure 4A); while the jet-milled ciprofloxacin particles were small with rough surfaces and irregular shapes (Figure 4B). Raw MgSt (Figure 4C) showed flake-like particles, and the co-milled MgSt/ciprofloxacin (Figure 4D) had similar surface features to the jet-milled ciprofloxacin particles (Figure 4A). Micronized L-leucine (Figure 4E) appeared as polydispersed rough particles. Small particles seem to form rough surfaces on ciprofloxacin particles after co-jet-milling (Figure 4F). These images suggest that the coating patterns with two lubricants could be different, which may explain their different aerosolization-enhancer behaviour.

3.7 Effect of Jet-milling Process Parameters

3.7.1 Number of jet-milling cycles—We chose 5% w/w lubricant for further investigation of the effects of co-jet-milling processing parameters (Figure 5), because further increase in the lubricant concentration did not improve aerosolization significantly. Interestingly, the FPF of those formulations processed with MgSt and L-leucine decreased substantially after an additional jet-milling cycle.

3.7.2 Feed and grinding pressures—In a jet-mill, feed and grinding pressures control the shear applied and hence may affect the aerosol performance (Lau et al., 2017b). Therefore, the aerosol performance of ciprofloxacin co-jet-milled at varying feeding and grinding pressures was assessed. Figure 6 shows the FPF of ciprofloxacin co-jet-milled with different lubricants at various feeding and grinding pressures. It was noted that the grinding and feed pressure did not affect the FPF of ciprofloxacin co-jet-milled with MgSt ($p>0.05$).

Ciprofloxacin co-jet-milled with L-leucine showed only a slight reduction in FPF at lower feeding and grinding pressures as compared with the Feed:Grinding Pressure_6:5 bar ($p<0.05$).

3.8 Carr's index and cohesion

Table 3 shows bulk and tap densities, Carr's index and cohesion data of the selected ciprofloxacin samples. Typically, a high bulk density and/or a low Carr's index are indicative of better packing attributable to lower cohesiveness. Our results show that Carr's index of the jet-milled ciprofloxacin was relatively high, and the co-jet-milling with 5% w/w lubricants substantially reduced the Carr's index values (Table 3). The Carr's index values of ciprofloxacin co-jet-milled with 5% w/w MgSt and 5% w/w L-leucine were not significantly different ($p > 0.05$). Considering bulk and tap densities, significant increases are seen for 5% MgSt, while 5% L-leucine did not change the bulk and tap densities as compared with the pure jet-milled ciprofloxacin.

The cohesion measured by shear shell indicated that jet-milled ciprofloxacin had a relatively high cohesion, and MgSt substantially reduced the cohesion of ciprofloxacin (Table 3). Interestingly, L-leucine showed no effect on the cohesion of ciprofloxacin. The low value for MgSt is in accordance with the bulk and tap densities data. It is worth noting that the Carr's index and the shear cell measure different properties: Typically, the Carr's index is calculated by poured and tapped densities while shear cell testing assesses movement capability of powder beds under the consolidated conditions (Tan et al., 2015). In summary, the 5% MgSt formulation has shown better flow as indicated by densities and cohesion values as compared with the ciprofloxacin jet-milled alone and 5% L-Leucine formulations (Tan et al., 2015).

3.9 *In vitro* dissolution

The dissolution kinetics of selected samples were determined using both the beaker method (Figure 7A) and the Franz diffusion method (Figure 7B).

In the beaker method, for all the samples, more than 80% of ciprofloxacin was dissolved within 5 minutes (Figure 7A) indicating lubricants had no deleterious effect on the dissolution kinetics of ciprofloxacin.

The Franz cell data showed relatively slower dissolution rates as compared to the results measured by the beaker method. As with the Franz cell method, in general the ciprofloxacin samples co-jet-milled with lubricants showed no substantial decrease in the release rate as compared with the jet-milled ciprofloxacin alone. The only statistically significant retarded dissolution rates were found for 5% leucine-coated formulations at 45 and 60 mins as compared to the jet-milled ciprofloxacin alone ($p < 0.05$). The data have shown coating with L-leucine has some minor influence on Franz cell dissolution, likely due to the impact on permeation of the drug through the Franz cell membrane.

4. Discussion

Dry powder formulations have been developed for high-dose inhalation products due to the ease of administration compared with the liquid-based therapeutic aerosols (Hickey et al., 2007). However, the cohesive nature of jet-milled powders compromises the aerosolization and poses a significant challenge to deliver high–dose drugs to the lungs (Hoppentocht et al., 2014; Jong et al., 2016; Louey et al., 2004). Co-jet-milling with lubricants may enable simultaneous particle size reduction and dry coating, producing powders with improved aerosol performance (Lau et al., 2017b). In this study, for the first time we establish the correlations between surface coating coverage and aerosolization performance after co-jet-milling with lubricants and elucidate the different mechanisms that promote aerosolization for MgSt and L-leucine.

Our results clearly show that co-jet-milling significantly improved the aerosolization of ciprofloxacin with a L-leucine concentration of 0.5% w/w and MgSt concentration of 5%, respectively. The surface concentrations of lubricants measured by XPS were higher than their theoretical corresponding formulation concentrations, indicating that lubricant materials coat the drug particles during co-jet-milling, rather than just being physical mixtures. It is interesting to note that an increase in the lubricant concentration from 0.5% to 1% did not lead to further improved FPF for either L-leucine or MgSt. We hypothesized that this was due to the unchanged surface coverage of lubricants on the co-jet-milled particles between 0.5% and 1% lubricants, because the coverage of lubricant coating has a crucial influence on the inter-particle interactions and hence aerosolization performance for fine inhalation drug particles (Zhou et al., 2013). To test such a hypothesis, the surface composition of the selected samples was characterized qualitatively and quantitatively using ToF-SIMS and XPS with an aim to establish the relationship between aerosolization and surface lubricant coverage. Indeed, XPS data demonstrated that when L-leucine and MgSt concentrations increased from 0.5% - 1% in the formulations, surface coverage of lubricants did not change significantly ($p > 0.05$), which was corresponding to the unchanged FPF. Furthermore, we established the correlations between surface lubricant coverage and FPF for both MgSt and L-leucine. Figure 8 indicated clear correlations between surface lubricant coverage and FPF for MgSt ($R^2 = 0.897$) and L-leucine ($R^2 = 0.847$) in the tested surface coverage range. Such quantitative correlations provided a better understanding on how surface coating critically impacts aerosolization.

Another important finding of this study is that the improvement in aerosolization is material-dependent. Previous studies have indicated that MgSt typically exhibits better delamination efficiency than L-leucine (Morton and Staniforth, 2005; Morton et al., 2005; Wei et al., 2017). Interestingly, the FPF achieved with L-leucine was higher when compared with that of MgSt at corresponding concentrations, while the surface coverage of L-leucine was significantly lower than MgSt as measured by XPS. In our earlier study, we have revealed the different coating mechanisms of MgSt and L-leucine for improving powder flow of larger drug particles (approximately 25 μm) : MgSt tends to delaminate into a coating film so as to reduce surface energy; L-leucine tends to form rougher surfaces and reduced contact area (Qu et al., 2015b). Such differences could also be the distinguishing mechanisms to improve aerosolization in the current study; though the coating approaches and drug

particles are different in the two studies. XPS and ToF-SIMS have demonstrated the varying coating patterns/levels between these two lubricants. At the same concentration, MgSt led to higher coating coverage than L-leucine. Furthermore, surface energy data also support our hypothesis. A lower surface energy in general represents lower interparticle forces and improved aerosol performance (Saleem et al., 2008). The surface energies of MgSt-processed samples are lower than those of L-leucine-processed samples; however, L-leucine-processed samples have better aerosol performance. In addition, there is no apparent difference in surface energy between L-leucine-processed formulations with different lubricant concentrations (and different lubricant surface coverage); but the surface energy of MgSt-processed samples is highly dependent on the lubricant concentration or surface lubricant coverage. These surface energy data provide evidence that MgSt-coating relies on film formation or surface coverage to improve aerosolization via reduced surface energy, but not for L-leucine coating. This is further supported by bulk and tap density data, and by cohesion data measured with the shear cell, all pointing to a lowered cohesion in the 5% MgSt-coated system. SEM images also suggest that there are more ultra-fine nanometer-scale particles on the L-leucine coated particles than on the MgSt coated particles. In summary, all the collective data suggest different mechanisms to improve aerosolization after co-jet milling ciprofloxacin with MgSt and L-leucine. The fact that L-leucine coating shows better FPF performance as compared to MgSt coating at the same excipient concentration suggests that factors other than surface energy reduction are also crucial to the FPF, such as the surface rugosity produced by L-leucine coating in this study.

There may be a concern regarding dissolution behavior of drug particles coated with hydrophobic materials such as MgSt (Nokhodchi et al., 2009). Our study shows that there is no substantial change in dissolution rate for ciprofloxacin, a water-soluble drug, when it was co-jet-milled with 5% w/w MgSt. This is in agreement with our previous findings with larger particles for oral dosage forms (Qu et al., 2017; Qu et al., 2015a; Qu et al., 2015b; Wei et al., 2017). This is likely due to the incomplete coating after co-jet-milling; the surface coverages of 5% MgSt measured by XPS were only 32.7 ± 4.8 (Qu et al., 2015b).

5. Conclusions

This study provides quantitative correlations between surface lubricant coverage and aerosolization performance of co-jet-milled ciprofloxacin particles. Our results demonstrated that co-jet-milling with MgSt and L-leucine resulted in simultaneous size reduction and surface coating of ciprofloxacin particles, and such coating entailed significant improvements in aerosolization. Co-jet-milling of ciprofloxacin particles with 5% w/w hydrophobic MgSt did not retard dissolution due the discontinuous nature of the coating. More importantly, we have discovered the different mechanisms between MgSt and L-leucine coating to improve aerosolization by co-jet-milling. MgSt coating acts primarily by reducing the surface energy and the friction between particles and yields a higher surface coverage than L-leucine at the corresponding concentration. L-leucine coating has less effect on the surface energy, but seems to create more rough surfaces, thereby reducing inter-particulate contact area and hence total inter-particulate attractive force. Our findings have shown the coating structure and quality and their effects can be highly dependent on the process and the coating material. These findings provide fundamental understanding of the

critical effects of MgSt and L-leucine surface coverages on aerosolization and powder flow properties of inhalation particles.

Acknowledgments

Research reported in this publication was partially supported by the Dane O. Kildsig Center for Pharmaceutical Processing Research (CPPR). Qi (Tony) Zhou was supported by the National Institute of Allergy and Infectious Diseases of the National Institutes of Health under Award Number R01AI132681. The content is solely the responsibility of the authors and does not necessarily represent the official views of the National Institutes of Health. The authors are grateful for the scientific and technical assistance of the Australian Microscopy & Microanalysis Research Facility at the Future Industries Institute, University of South Australia. Kind donations of RS01 DPI device from Plastiape S.p.A. and HPMC capsules from Qualicaps, Inc. are acknowledged.

References

Antoniu S, Azoicai D, 2013 Ciprofloxacin DPI in non-cystic fibrosis bronchiectasis: a Phase II randomized study. Expert opinion on investigational drugs 22, 671–673. [PubMed: 23516961]

Begat P, Price R, Harris H, Morton DA, Staniforth JN, 2005 The influence of force control agents on the cohesive-adhesive balance in dry powder inhaler formulations. KONA Powder and Particle Journal 23, 109–121.

Bhujbal SV, Zemlyanov DY, Cavallaro A, Mangal S, Taylor LS, Zhou QT, 2018 Qualitative and Quantitative Characterization of Composition Heterogeneity on the Surface of Spray Dried Amorphous Solid Dispersion Particles by an Advanced Surface Analysis Platform with High Surface Sensitivity and Superior Spatial Resolution. Molecular pharmaceutics 15, 2045–2053. [PubMed: 29641898]

Carr R, 1965 Evaluating flow properties of solids. Chemical engineering science 72, 163–168.

Chan HK, Chew NY, 2003 Novel alternative methods for the delivery of drugs for the treatment of asthma. Advanced drug delivery reviews 55, 793–805. [PubMed: 12842601]

Cheah SE, Wang J, Nguyen VT, Turnidge JD, Li J, Nation RL, 2015 New pharmacokinetic/pharmacodynamic studies of systemically administered colistin against Pseudomonas aeruginosa and Acinetobacter baumannii in mouse thigh and lung infection models: smaller response in lung infection. The Journal of antimicrobial chemotherapy 70, 3291–3297. [PubMed: 26318190]

Cipolla D, Chan H-K, 2013 Inhaled antibiotics to treat lung infection. Pharmaceutical Patent Analyst 2, 647–663. [PubMed: 24237172]

Das SC, Larson I, Morton DAV, Stewart PJ, 2011 Determination of the polar and total surface energy distributions of particulates by inverse gas chromatography. Langmuir 27, 521–523. [PubMed: 21174410]

Fowkes FM, 1964 Attractive forces at interfaces. Industrial & engineering chemistry research 56, 40–52.

Frijlink H, De Boer A, 2004 Dry powder inhalers for pulmonary drug delivery. Expert opinion on drug delivery 1, 67–86. [PubMed: 16296721]

Giry K, Pean JM, Giraud L, Marsas S, Rolland H, Wuthrich P, 2006 Drug/lactose comicronization by jet milling to improve aerosolization properties of a powder for inhalation. International journal of pharmaceutics 321, 162–166. [PubMed: 16797150]

Healy AM, Amaro MI, Paluch KJ, Tajber L, 2014 Dry powders for oral inhalation free of lactose carrier particles. Advanced drug delivery reviews 75, 32–52. [PubMed: 24735676]

Hickey A, Durham P, Dharmadhikari A, Nardell E, 2016 Inhaled drug treatment for tuberculosis: past progress and future prospects. Journal of Controlled Release 240, 127–134. [PubMed: 26596254]

Hickey AJ, Mansour HM, Telko MJ, Xu Z, Smyth HDC, Mulder T, McLean R, Langridge J, Papadopoulos D, 2007 Physical characterization of component particles included in dry powder inhalers. II. Dynamic characteristics. Journal of pharmaceutical sciences 96, 1302–1319. [PubMed: 17455364]

Hoppentocht M, Hagedoorn P, Frijlink HW, de Boer AH, 2014 Technological and practical challenges of dry powder inhalers and formulations. Advanced drug delivery reviews 75, 18–31. [PubMed: 24735675]

Jong T, Li J, Morton DA, Zhou QT, Larson I, 2016 Investigation of the changes in aerosolization behavior Between the jet-milled and spray-dried colistin powders through surface energy characterization. Journal of pharmaceutical sciences 105, 1156–1163. [PubMed: 26886330]

Kou X, Chan LW, Steckel H, Heng PW, 2012 Physico-chemical aspects of lactose for inhalation. Advanced drug delivery reviews 64, 220–232. [PubMed: 22123598]

Lau M, Young PM, Traini D, 2017a Co-milled API-lactose systems for inhalation therapy: impact of magnesium stearate on physico-chemical stability and aerosolization performance. Drug development and industrial pharmacy 43, 980–988. [PubMed: 28122460]

Lau M, Young PM, Traini D, 2017b A review of co-milling techniques for the production of high dose dry powder inhaler formulation. Drug development and industrial pharmacy 43, 1229–1238. [PubMed: 28367654]

Lin Y-W, Zhou QT, Cheah S-E, Zhao J, Chen K, Wang J, Chan H-K, Li J, 2017a Pharmacokinetics/pharmacodynamics of pulmonary delivery of colistin against Pseudomonas aeruginosa in a mouse lung infection model. Antimicrobial agents and chemotherapy 61, e02025–02016. [PubMed: 28031207]

Lin Y-W, Zhou QT, Han M-L, Onufrak NJ, Chen K, Wang J, Forrest A, Chan H-K, Li J, 2018 Mechanism-based pharmacokinetic/pharmacodynamic modeling of aerosolized colistin in a mouse lung infection model. Antimicrobial agents and chemotherapy 62, e01965–01917. [PubMed: 29263069]

Lin Y-W, Zhou QT, Hu Y, Onufrak NJ, Sun S, Wang J, Forrest A, Chan H-K, Li J, 2017b Pulmonary pharmacokinetics of colistin following administration of dry powder aaerosols in rats. Antimicrobial agents and chemotherapy 61, e00973–00917. [PubMed: 28807905]

Lin YW, Wong J, Qu L, Chan HK, Zhou QT, 2015 Powder production and particle engineering for dry powder inhaler formulations. Current pharmaceutical design 21, 3902–3916. [PubMed: 26290193]

Louey MD, Van Oort M, Hickey AJ, 2004 Aerosol dispersion of respirable particles in narrow size distributions produced by jet-milling and spray-drying techniques. Pharmaceutical research 21, 1200–1206. [PubMed: 15290860]

Mangal S, Nie H, Xu R, Guo R, Cavallaro A, Zemlyanov D, Zhou QT, 2018 Physico-chemical properties, aerosolization and dissolution of co-spray dried azithromycin particles with L-Leucine for inhalation. Pharmaceutical research 35, 28. [PubMed: 29374368]

Mangal S, Xu R, Park H, Zemlyanov D, Shetty N, Lin Y-W, Morton D, Chan H-K, Li J, Zhou QT, 2019 Understanding the Impacts of Surface Compositions on the In-Vitro Dissolution and Aerosolization of Co-Spray-Dried Composite Powder Formulations for Inhalation. Pharmaceutical research 36, 6.

May S, Jensen B, Wolkenhauer M, Schneider M, Lehr CM, 2012 Dissolution Techniques for In Vitro Testing of Dry Powders for Inhalation. Pharmaceutical research 29, 2157–2166. [PubMed: 22528980]

Miller DP, Tan T, Tarara TE, Nakamura J, Malcolmson RJ, Weers JG, 2015 Physical characterization of tobramycin inhalation powder: I. rational design of a stable engineered-particle formulation for delivery to the lungs. Molecular pharmaceutics 12, 2582–2593. [PubMed: 26052676]

Morton D, Staniforth J, 2005 Dry powder composition comprising co-jet milled particles for pulmonary inhalation. US patent application US20060257491A1 Google Patents.

Morton D, Staniforth J, Tobyn M, Eason S, Harmer Q, Ganderton D, 2005 Pharmaceutical compositions for treating premature ejaculation by pulmonary inhalation. WO patent application WO2005025550A1 Google Patents.

Musa R, Ventura P, Chiesi P, 2000 Improved powdery pharmaceutical compositions for inhalation. WO Application WO2000053157A1 Google Patents.

Nokhodchi A, Okwudarue ON, Valizadeh H, Momin MN, 2009 Cogrinding as a Tool to Produce Sustained Release Behavior for Theophylline Particles Containing Magnesium Stearate. AAPS PharmSciTech 10, 1243. [PubMed: 19862623]

Pilcer G, Amighi K, 2010 Formulation strategy and use of excipients in pulmonary drug delivery. International Journal of Pharmaceutics 392, 1–19. [PubMed: 20223286]

Qu L, Stewart PJ, Hapgood KP, Lakio S, Morton DA, Zhou QT, 2017 Single-step Coprocessing of Cohesive Powder via Mechanical Dry Coating for Direct Tablet Compression. Journal of pharmaceutical sciences 106, 159–167. [PubMed: 27665128]

Qu L, Zhou Q, Gengenbach T, Denman JA, Stewart PJ, Hapgood KP, Gamlen M, Morton DA, 2015a Investigation of the potential for direct compaction of a fine ibuprofen powder dry-coated with magnesium stearate. Drug development and industrial pharmacy 41, 825–837. [PubMed: 24738790]

Qu L, Zhou QT, Denman JA, Stewart PJ, Hapgood KP, Morton DA, 2015b Influence of coating material on the flowability and dissolution of dry-coated fine ibuprofen powders. European Journal of Pharmaceutical Sciences 78, 264–272. [PubMed: 26215464]

Salama RO, Traini D, Chan H-K, Young PM, 2008 Preparation and characterisation of controlled release co-spray dried drug–polymer microparticles for inhalation 2: Evaluation of in vitro release profiling methodologies for controlled release respiratory aerosols. European Journal of Pharmaceutics and Biopharmaceutics 70, 145–152. [PubMed: 18534832]

Saleem I, Smyth H, Telko M, 2008 Prediction of dry powder inhaler formulation performance from surface energetics and blending dynamics. Drug development and industrial pharmacy 34, 1002–1010. [PubMed: 18686090]

Schultz J, Lavielle L, Martin C, 1987 The role of the interface in carbon fibre-epoxy composites. Journal of adhesion 23, 45–60.

Schulze D, 2008 Powders and bulk solids: behavior, characterization, storage and flow Springer, Berlin.

Schwarz C, 2015 Colobreathe® for the treatment of cystic fibrosis-associated pulmonary infections. Pulmonary Therapy 1, 19–30.

Shetty N, Ahn P, Park H, Bhujbal S, Zemlyanov D, Cavallaro A, Mangal S, Li J, Zhou QT, 2018 Improved physical stability and aerosolization of inhalable amorphous ciprofloxacin powder formulations by incorporating synergistic colistin. Mol Pharm 15, 4004–4020. [PubMed: 30028947]

Staniforth JN, Morton D, Tobyn M, Eason S, Harmer Q, Ganderton D, 2004 Pharmaceutical compositions comprising apomorphine for pulmonary inhalation. WO Application WO2004089374A1 Google Patents.

Stank K, Steckel H, 2013 Physico-chemical characterisation of surface modified particles for inhalation. International journal of pharmaceutics 448, 9–18. [PubMed: 23518364]

Steckel H, Stank K, 2014 Powder processing: performance improvements through co-milling, Respiratory Drug Delivery.

Tan G, Morton DA, Larson I, 2015 On the methods to measure powder flow. Current pharmaceutical design 21, 5751–5765. [PubMed: 26446467]

Telko MJ, Hickey AJ, 2005 Dry powder inhaler formulation. Respiratory care 50, 1209–1227. [PubMed: 16122404]

van Oss CJ, Chaudhury MK, Good RJ, 1987 Monopolar surfaces. Advances in colloid and interface science 28, 35–64. [PubMed: 3333137]

Velkov T, Abdul Rahim N, Zhou Q, Chan H-K, Li J, 2015 Inhaled anti-infective chemotherapy for respiratory tract infections: Successes, challenges and the road ahead. Advanced Drug Delivery Reviews 85, 65–82. [PubMed: 25446140]

Wang W, Zhou QT, Sun S-P, Denman JA, Gengenbach TR, Barraud N, Rice SA, Li J, Yang M, Chan H-K, 2016 Effects of Surface Composition on the Aerosolisation and Dissolution of Inhaled Antibiotic Combination Powders Consisting of Colistin and Rifampicin. The AAPS Journal 18, 372–384. [PubMed: 26603890]

Wei G, Mangal S, Denman J, Gengenbach T, Lee Bonar K, Khan RI, Qu L, Li T, Zhou QT, 2017 Effects of coating materials and processing conditions on flow enhancement of cohesive acetaminophen powders by high-shear processing with pharmaceutical lubricants. Journal of pharmaceutical sciences 106, 3022–3032. [PubMed: 28551425]

Yla-Maihaniemi P, Heng J, Thielmann F, Williams D, 2008 Inverse gas chromatographic method for measuring the dispersive surface energy distribution for particulates. Langmuir 24, 9551–9557. [PubMed: 18680326]

Zhou Q, Leung SSY, Tang P, Parumasivam T, Loh ZH, Chan H-K, 2015 Inhaled formulations and pulmonary drug delivery systems for respiratory infections. Advanced Drug Delivery Reviews 85, 83–99. [PubMed: 25451137]

Zhou Q, Qu L, Gengenbach T, Larson I, Stewart P, Morton DV, 2013 Effect of surface coating with magnesium stearate via mechanical dry powder coating approach on the aerosol performance of micronized drug powders from dry powder inhalers. AAPS PharmSciTech 14, 38–44. [PubMed: 23196863]

Zhou QT, Denman JA, Gengenbach T, Das S, Qu L, Zhang H, Larson I, Stewart PJ, Morton DA, 2011 Characterization of the surface properties of a model pharmaceutical fine powder modified with a pharmaceutical lubricant to improve flow via a mechanical dry coating approach. Journal of pharmaceutical sciences 100, 3421–3430. [PubMed: 21455980]

Zhou QT, Qu L, Larson I, Stewart PJ, Morton DAV, 2010 Improving aerosolization of drug powders by reducing powder intrinsic cohesion via a mechanical dry coating approach. International journal of pharmaceutics 394, 50–59. [PubMed: 20435112]

Zhou QT, Tang P, Leung SSY, Chan JGY, Chan H-K, 2014 Emerging inhalation aerosol devices and strategies: where are we headed? Advanced drug delivery reviews 75, 3–17. [PubMed: 24732364]

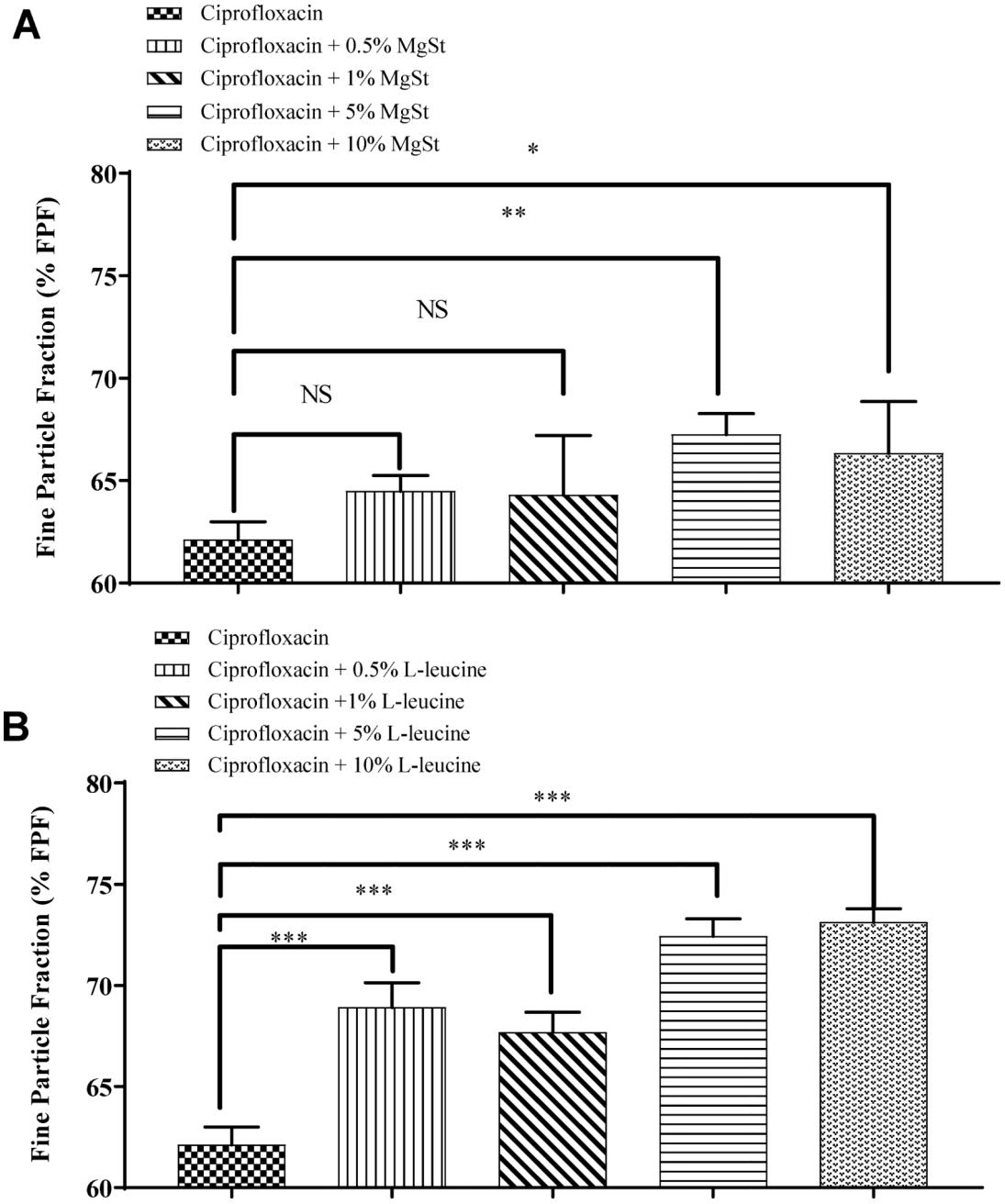

Figure 1:

Effects of MgSt (A) and L-leucine (B) on the % fine particle fraction (FPF) of jet-milled ciprofloxacin. The data are presented as mean ± SD (n=4). * Significantly different from ciprofloxacin jet-milled alone, $p < 0.05$, ** Significantly different from ciprofloxacin jet-milled alone, $p < 0.01$, *** Significantly different from ciprofloxacin jet-milled alone, $p < 0.001$, NS no significance from ciprofloxacin jet-milled alone, $p > 0.05$.

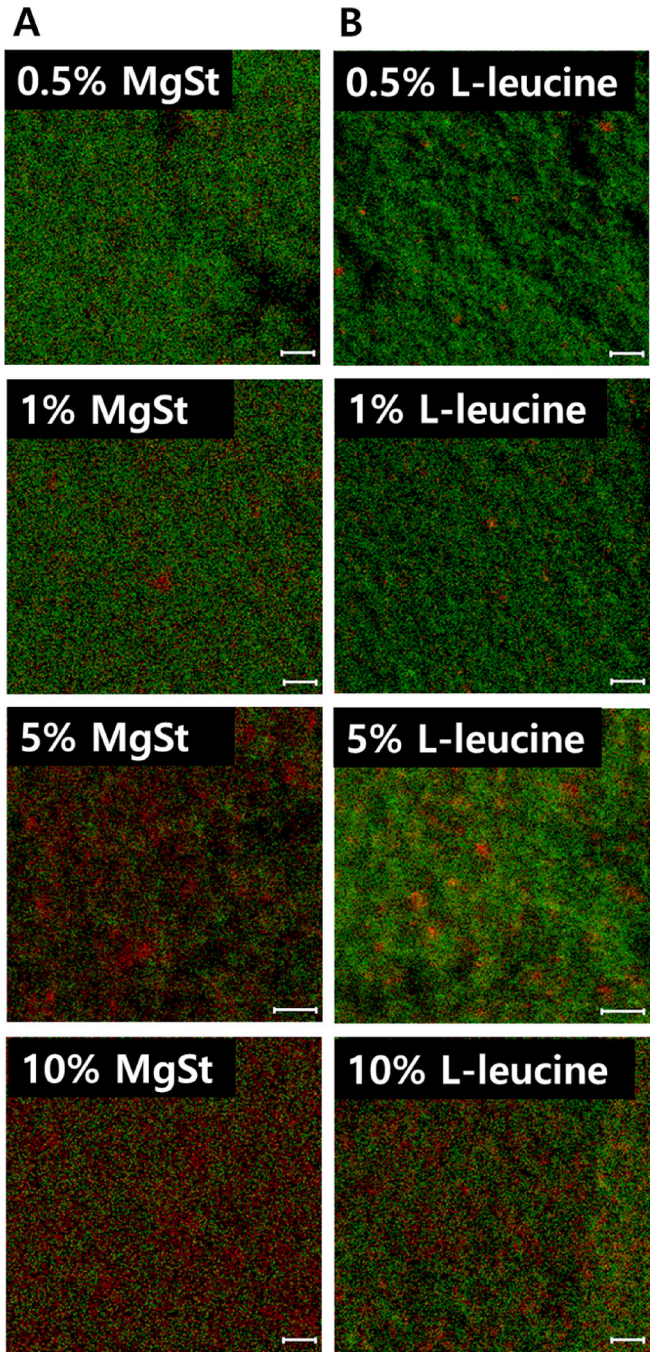

Figure 2:
Distributions of the coating material (red) on the surfaces of co-jet-milled ciprofloxacin particles (green) with (A) MgSt and (B) L-leucine (scale bar represents 10 μm).

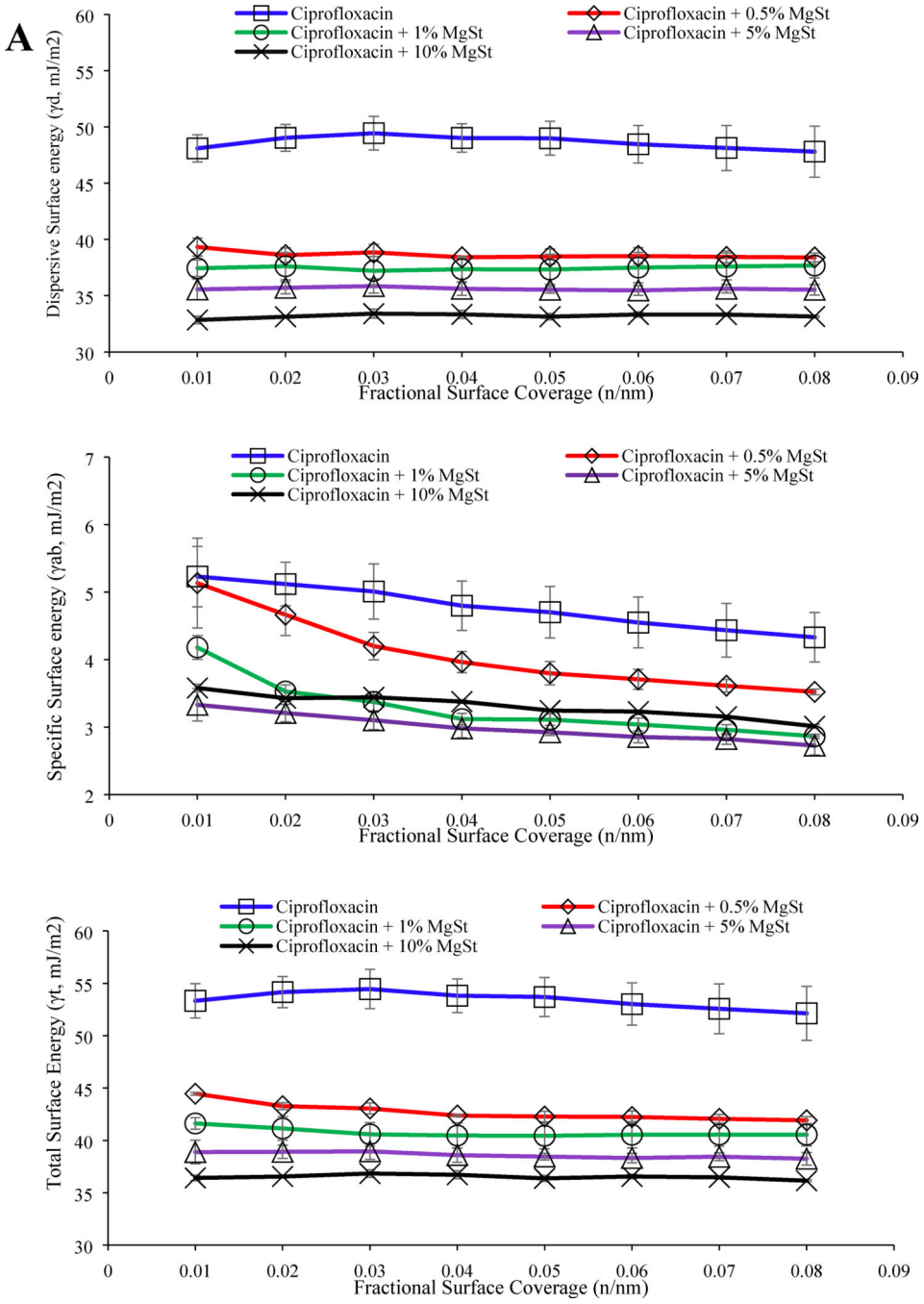

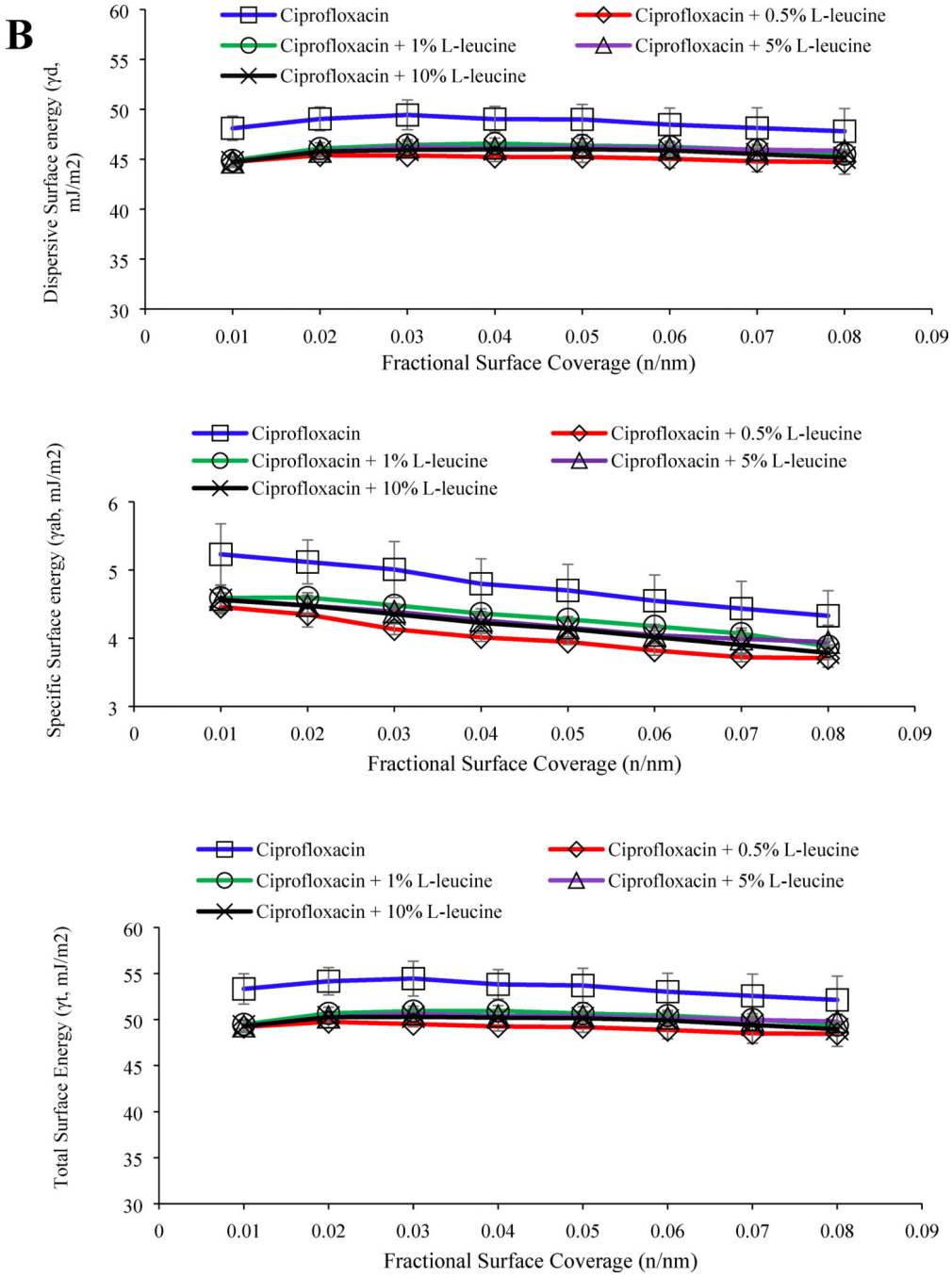

Figure 3:

Dispersive, specific and total surface energy data of jet-milled ciprofloxacin with (A) MgSt and (B) L-leucine. The data are presented as mean ± SD (n=3).

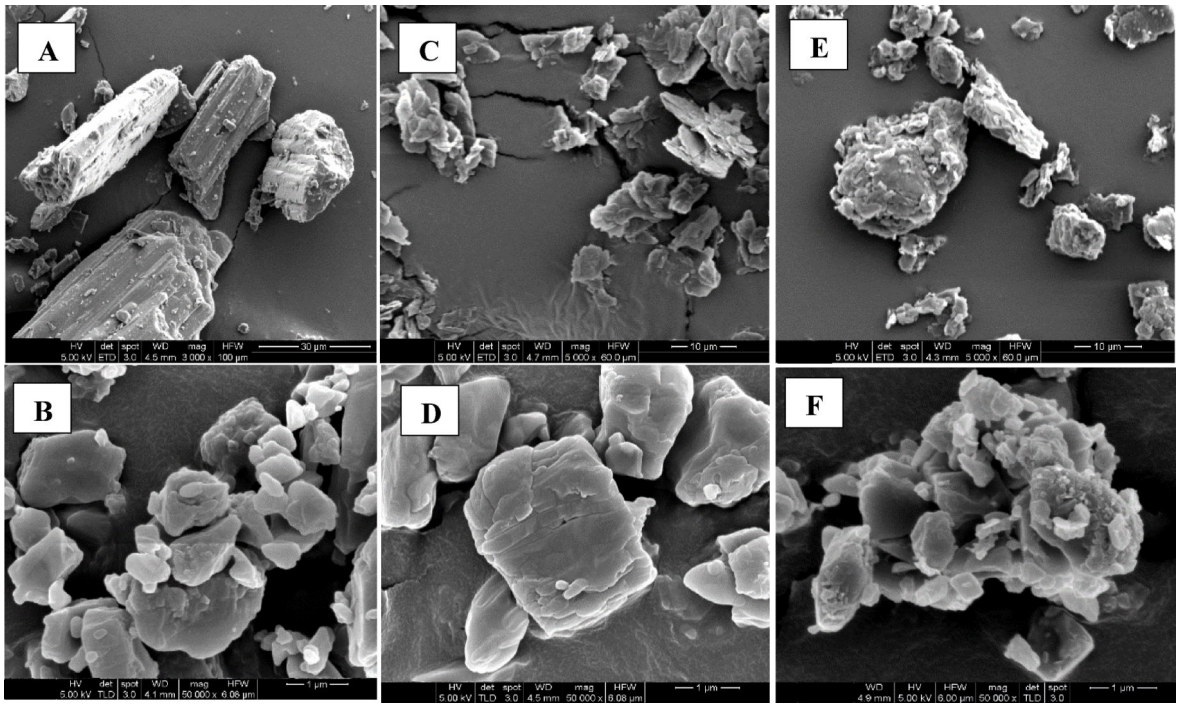

Figure 4:

Representative SEM images of (A) raw ciprofloxacin, (B) jet-milled ciprofloxacin, (C) raw MgSt (D) co-jet-milled ciprofloxacin + 5% w/w MgSt, (E) ball-milled L-leucine (F) co-jet-milled ciprofloxacin + 5% w/w L-leucine. The co-jet-milled samples are produced at grinding and feed pressures of 5 and 6 bar, respectively.

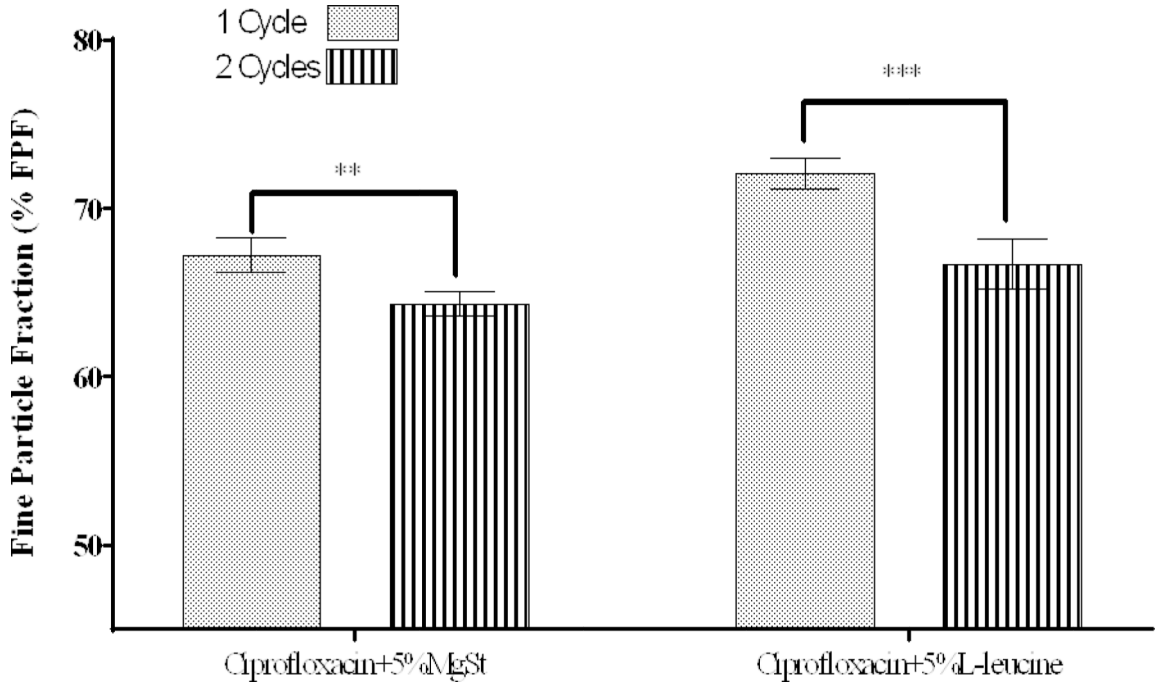

Figure 5:

Effect of number of jet-milling cycles on the % fine particle fraction (FPF) of ciprofloxacin co-jet-milled with L-leucine or MgSt. The data are presented as mean ± SD (n=4). ** Significantly different, $p < 0.01$, *** Significantly different, $p < 0.001$.

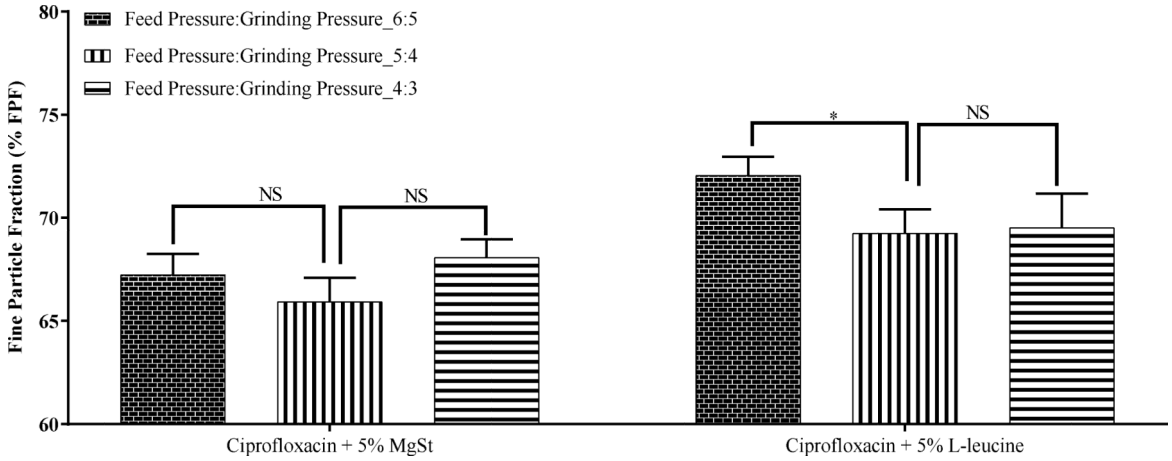

Figure 6:

Effect of feed and grinding pressures (bar) on the fine particle fraction (FPF) of ciprofloxacin co-jet-milled with different lubricants. The data are presented as mean ± SD (n=4). * Significant difference, $p < 0.05$, NS, no significant difference.

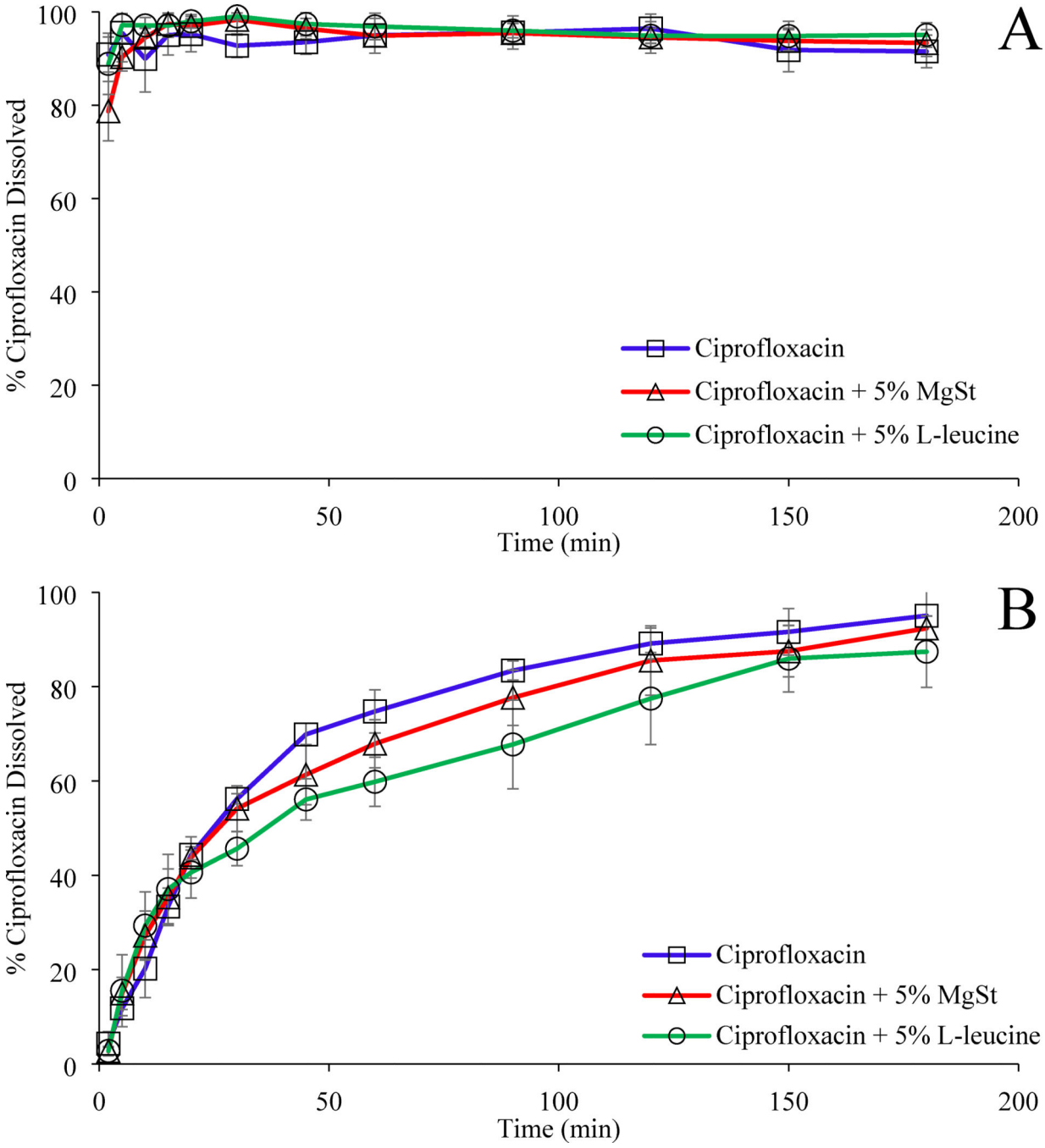

Figure 7:

In vitro dissolution of ciprofloxacin from the selected formulations determined using beaker method (A) and Franz diffusion method (B). The data are presented as mean ± SD (n=4).

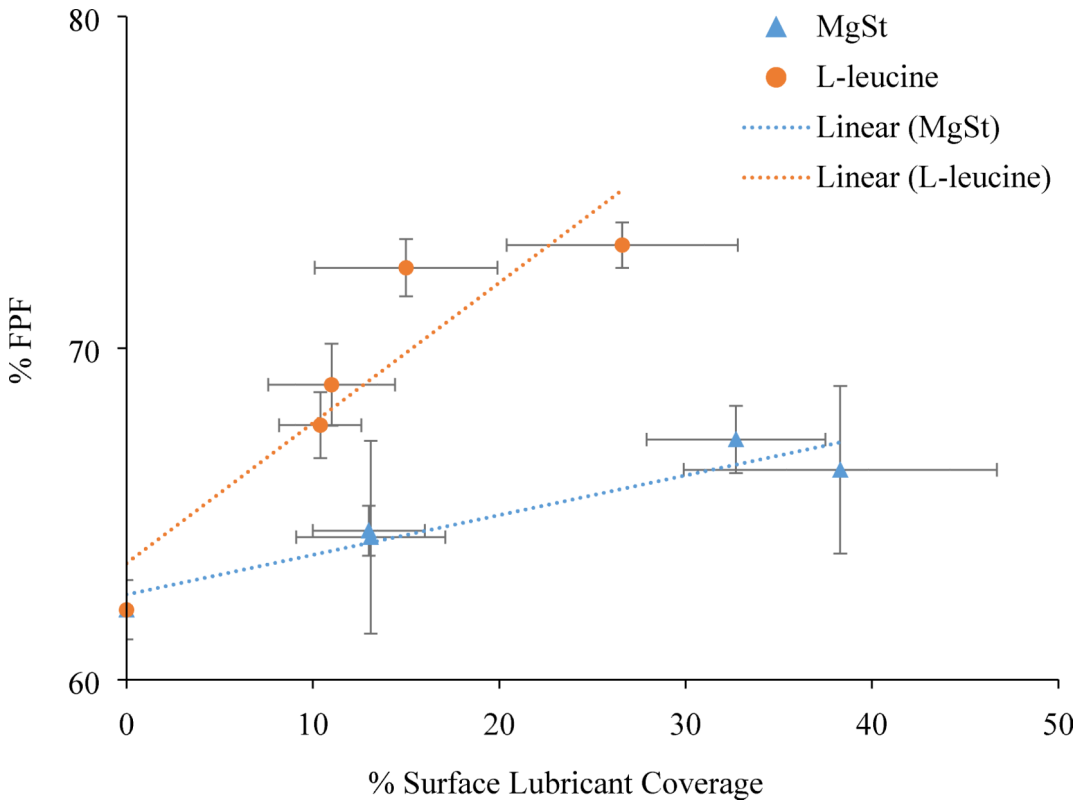

Figure 8:

Correlations between surface coverage of lubricants (as determined by XPS) and fine particle fraction (FPF) of the jet-milled ciprofloxacin samples with lubricants of (A) MgSt and (B) L-leucine. The data are presented as mean ± SD (n=4).

Table 1:

Particle sizes of the selected jet-milled ciprofloxacin samples (n=3).

		D_{10} (μm)	D_{50} (μm)	D_{90} (μm)	Span
Ciprofloxacin	Mean	1.0	2.0	4.9	2.0
	SD	0.0	0.0	0.7	0.3
Ciprofloxacin + 0.5% MgSt	Mean	0.9**	1.9**	4.4	1.9
	SD	0.0	0.0	0.1	0.1
Ciprofloxacin + 1% MgSt	Mean	0.9**	1.9**	4.7	2.0
	SD	0.0	0.0	0.3	0.1
Ciprofloxacin + 5% MgSt	Mean	0.9**	1.8**	3.7*	1.6
	SD	0.0	0.0	0.1	0.0
Ciprofloxacin + 10% MgSt	Mean	0.9**	1.9**	4.3	1.8
	SD	0.0	0.0	0.0	0.0
Ciprofloxacin + 0.5% L-leucine	Mean	1.0	2.0	4.0	1.6
	SD	0.0	0.0	0.0	0.0
Ciprofloxacin + 1% L-leucine	Mean	1.0**	1.9	3.7*	1.4*
	SD	0.0	0.0	0.1	0.0
Ciprofloxacin + 5% L-leucine	Mean	0.9	1.9**	3.8*	1.5*
	SD	0.0	0.0	0.01	0.0
Ciprofloxacin + 10% L-leucine	Mean	0.9	1.8**	3.5**	1.4**
	SD	0.0	0.0	0.1	0.0

* Significantly different from ciprofloxacin jet-milled alone, $p < 0.05$

** Significantly different from ciprofloxacin jet-milled alone, $p < 0.01$

Table 2:

Effect of lubricant concentration and lubricant materials on the surface coverage of co-jet-milled ciprofloxacin powders determined by XPS (based on C 1s curvefit, n=6).

Formulations (w/w %)	% Theoretical Surface Composition		% Measured Surface Composition	
	Ciprofloxacin	Lubricant	Ciprofloxacin	Lubricant
Ciprofloxacin + 0.5% MgSt	99.7	0.3	87.0 ± 3.0	13.0 ± 3.0
Ciprofloxacin + 1% MgSt	99.3	0.7	86.9 ± 4.0	13.1 ± 4.0
Ciprofloxacin + 5% MgSt	96.5	3.5	67.3 ± 4.8	32.7 ± 4.8
Ciprofloxacin + 10% MgSt	92.9	7.1	61.7 ± 8.4	38.3 ± 8.4
Ciprofloxacin + 0.5% L-leucine	99.5	0.5	89.0 ± 3.4	11.0 ± 3.4
Ciprofloxacin + 1% L-leucine	99.0	1.0	89.6 ± 2.2	10.4 ± 2.2
Ciprofloxacin + 5% L-leucine	94.8	5.2	85.0 ± 4.9	15.0 ± 4.9
Ciprofloxacin + 10% L-leucine	89.7	10.3	73.4 ± 6.2	26.6 ± 6.2

Table 3:

Densities, Carr's index and cohesion values of the selected jet-milled ciprofloxacin powders. The data are presented as mean ± SD (n=4).

	Bulk Density (g/mL)	Tapped Density (g/mL)	Carr's index	Cohesion (kPa)
Jet-milled ciprofloxacin	0.22 ± 0.03	0.34 ± 0.01	39.4 ± 1.6	3.7 ± 0.1
Co-jet-milled ciprofloxacin + 5% MgSt	0.29 ± 0.01 **	0.41 ± 0.01 **	29.1 ± 2.5 **	2.1 ± 0.3 **
Co-jet-milled ciprofloxacin + 5% L-leucine	0.23 ± 0.01	0.33 ± 0.01	32.6 ± 1.3 **	3.8 ± 0.3

** Significantly different compared to ciprofloxacin jet-milled alone, $p < 0.01$